Overcoming tumor resistance to cisplatin through micelles mediated combination chemotherapy

Journal:	*Biomaterials Science*
Manuscript ID:	BM-ART-08-2014-000305.R1
Article Type:	Paper
Date Submitted by the Author:	04-Sep-2014

Complete List of Authors:	Zhou, Dongfang; Changchun Institute of Applied Chemistry, Polymer chemistry Cong, Yuwei; Changchun Institute of Applied Chemistry, Polymer chemistry Qi, Yanxin; Changchun Institute of Applied Chemistry, Polymer chemistry Xiong, Hejian; Changchun Institute of Applied Chemistry, Polymer chemistry He, Shasha; Changchun Institute of Applied Chemistry, Polymer chemistry Wu, Yanjuan; State Key Laboratory of Polymer Physics and Chemistry, Changchun Institute of Applied Chemistry, Chinese Academy of Sciences, ; Graduate University of the Chinese Academy of Sciences, Xie, Zhigang; State Key Laboratory of Polymer Physics and Chemistry, Changchun Institute of Applied Chemistry, Chinese Academy of Sciences, Chen, Xuesi; Chinese Academy of Sciences,Changchun Institute of Applied Chemistry, Key Laboratory of Polymer Ecomaterials, Jing, Xiabin; State Key Laboratory of Polymer Physics and Chemistry, Changchun Institute of Applied Chemistry, Chinese Academy of Sciences, Huang, Yubin; Changchun Institute of Applied Chemistry, Polymer chemistry

Journal Name

RSCPublishing

ARTICLE

Overcoming tumor resistance to cisplatin through micelles mediated combination chemotherapy

Cite this: DOI: 10.1039/xoxxoooooox

Dongfang Zhou,[a] Yuwei Cong,[a,b] Yanxin Qi,[a] Shasha He,[a,b] Hejian Xiong,[a,b] Yanjuan Wu,[a,b] Zhigang Xie,[a] Xuesi Chen,[c] Xiabin Jing,[a] and Yubin Huang*[a]

Received ooth January 2012,
Accepted ooth January 2012

DOI: 10.1039/xoxxoooooox

www.rsc.org/

The main obstacles to cancer therapy are the inability to target cancer cells and the acquired drug resistance after a period of chemotherapy. Reduced drug uptake and DNA repair are the two main mechanisms involved in cisplatin resistance. In the present investigation, canthaplatin, a Pt (IV) pro-drug of cisplatin and a protein phosphatase 2A (PP2A) inhibitor (4-(3-carboxy-7-oxa-bicyclo[2.2.1] heptane-2-carbonyl)piperazine-1-carboxylic acid tertbutyl ester, LB), was designed and delivered using PEG-*b*-PLGA micelles for combination chemotherapy. Polymer/canthaplatin micelles facilitated the delivery of drugs into cancer cell through endocytosis and diminished DNA repair by PP2A inhibition, resulting in enhanced anti-tumor efficiency and excellent reversal ability on tumor resistance to cisplatin both *in vitro* and *in vivo*. Additionally, polymer/canthaplatin micelles could prolong drug residence in blood and decrease the side effects when compared to that of cisplatin.

Introduction

A major impediment for successful cancer therapy is drug's inability to target cancer cells and the side effect on normal cells. Most cancer therapies today are toxic to not only tumor but healthy tissues. And cancer patients often succumb to treatment more than disease. Furthermore, generation of drug resistance to external agents makes chemotherapy only work for short period. Platinum (II) compounds, cisplatin in particular, are employed in 50% of all cancer therapies, although accompanied with severe side effects and acquired resistance.[1-4] It's clear that novel paradigm is necessary to produce a safer and more effective cancer therapy using platinum.

Cisplatin has been put on numerous laboratory trials to minimize its side effects and increase cancer cell's susceptibility to it.[5,6] Several compounds such as mitaplatin and ethacraplatin have been developed to combine Pt (IV) pro-drugs with other chemotherapeutics for combination chemotherapy.[7,8] And some polymeric nano-carriers have also been explored for Pt (IV) pro-drugs delivery and combination chemotherapy.[9-16] Lippard co-encapsulated cisplatin and docetaxel in polymer nanoparticles to prostate cancer cells with synergistic cytotoxicity.[10] Mitaplatin was also encapsulated in PEG-PLGA nanoparticles through a double emulsion method.[13] Daunorubicin was reported to be delivered with oxaliplatin in co-assembled nanomicelles.[16] These systems demonstrated Pt-based drugs' potential attributes of improved tolerance and efficacy. However, it is still a challenge to overcome acquired tumor resistance to cisplatin both *in vitro* and *in vivo*.

Cisplatin sensitivity of cells correlates with DNA platination in that DNA is the ultimate target of cisplatin.[17] Tumor cells can be cisplatin-resistant, namely, they can achieve a reduction in the level of DNA platination through several mechanisms including reduced drug uptake, drug deactivation in cells, apoptosis inhibition and DNA repair.[18-21] Aiming at the two main mechanisms of cisplatin resistance, reduced drug uptake and DNA repair, we have previously reported a polymer-(tandem drugs) conjugate system with enhanced cancer treatment efficiency against malignant H22 tumor. In that system, a PP2A inhibitor demethylcantharidin (DMC) was combined with cisplatin to block DNA repair, and polymeric carriers were further used to deliver higher level drugs to cancer cells through endocytosis.[22] However, more results against cisplatin resistant cells

and tumors directly need to be demonstrated *in vitro* and *in vivo* to verify our strategy. Recently, LB, a DMC derivative with less toxicity and more PP2A inhibition specificity, demonstrated an impressive effect against a range of cancers in combination with temozolomide or doxorubicin.[23,24] It is reasonable that LB could be an attractive sensitizer when combined with cisplatin to combat cisplatin resistance.

Herein, we report a novel chemotherapeutic agent, canthaplatin, appending LB to cisplatin in a Pt (IV) pro-drug form. And canthaplatin was further encapsulated in PEG-*b*-PLGA nano-micelles (polymer/canthaplatin micelles) for polymeric combination chemotherapy. The drug loaded micelles could facilitate the delivery of canthaplatin into cancer cell through endocytosis and diminish DNA repair by PP2A inhibition of the intracellular reduced LB (Scheme 1). More importantly, tumor resistance to cisplatin was circumvented by polymer/canthaplatin micelles both *in vitro* and *in vivo*.

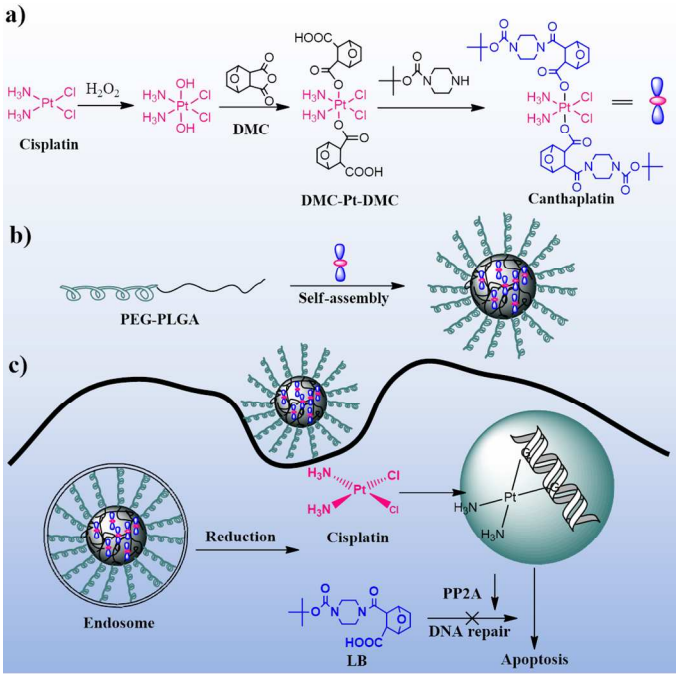

Scheme 1 a) Synthesis of canthaplatin, b) preparation of polymer/canthaplatin micelles and c) schematic representation of the intracellular action after endocytosis of polymer/canthaplatin micelles.

Materials and Methods

Materials

Hydrogen peroxide (H_2O_2), N, N'-carbonyldiimidazole (CDI), BOC-piperazine were purchased from Sigma-Aldrich. Cisplatin (purity 99.5%) was bought from Shandong Boyuan Chemical Company, China and demethylcantharidin (DMC) (purity 99%) was bought from Nanjing Zelang Biomedical Company, China. PEG_{5k}-*b*-$PLGA_{5k}$ and all other chemicals were purchased from Sigma-Aldrich and used as received.

General measurements

^{1}H NMR spectra were measured by a Unity-300 MHz NMR spectrometer (Bruker) at room temperature. Fourier transform infrared (FT-IR) spectra were recorded on a Bruker Vertex 70 spectrometer. Mass spectroscopy (ESI-MS) measurements were performed on a Quattro Premier XE system (Waters) equipped with an electrospray interface (ESI). Inductively coupled plasma optical emission spectrometer (ICP-OES, iCAP 6300, Thermoscientific, USA) was used to determine the total platinum contents in the micelles and samples obtained outside of the dialysis bags in drug release experiments. Inductively coupled plasma mass spectrometer (ICP-MS, Xseries II, Thermoscientific, USA) was used for quantitative determination of trace levels of platinum. Particle size and size distribution of micelles were determined by DLS with a vertically polarized HeeNe laser (DAWN EOS, Wyatt Technology, USA). The morphology of the polymer/canthaplatin micelles was measured by TEM performed on a JEOL JEM-1011 electron microscope. Clinic parameters were measured by an automatic biochemical analyzer (Mindray BS-220, China), and white blood concentration (WBC) was measured by an automatic blood counter system (ABX Micros 60, France). Flow cytometry (BD Biosciences) was used to determine whether treatment specifically induces apoptosis.

Preparation and characterization of polymer/canthaplatin micelles

Synthesis of canthaplatin. LB and DMC-Pt-DMC were synthesized according to references.[25,26] Canthaplatin was synthesized as follows: briefly, CDI (170 mg, 1.05 mmol) in dried DMF (16 mL) was added to a solution of DMC-Pt-DMC (335 mg, 0.5 mmol) in dried DMF (8 mL), and the mixture was heated to 60 °C. After 10 min stirring, the solution was cooled to room temperature and CO_2 was removed by flushing with argon. BOC-piperazine (195 mg, 1.05 mmol) in dried DMF (4 mL) was added drop-wise to the above solution and the mixture was left for 24 h at room temperature. DMF were removed under reduced pressure and water (50 mL) was then added, leaving a sticky white residue on the

flask wall. The light yellow aqueous solution was decanted and the residue was washed with water. The residue was triturated in excess diethyl ether, yielding canthaplatin as a white precipitate, which was filtered, washed with excess diethyl ether and recrystallised from THF/hexane (yield: 51.0 %; 256.7 mg). Canthaplatin was characterized using FTIR (Fig. S1), ^{1}H NMR (Fig. S2), ESI-MS (Fig. S3), and elemental analysis (Table S1).

Preparation of polymer/canthaplatin micelles. Micelles were prepared through a nano-precipitation process following a published protocol.[15] Briefly, 1 mg of PEG-*b*-PLGA and 1 mg of canthaplatin dissolved in acetonitrile were added drop-wise into deionized water under stirring. The resulting solution was then stirred at room temperature for 2 h and washed with an Amicon Ultra centrifugal filter (Millipore, Billerica, MA) with a molecular weight cutoff of 10 kDa， and then was freeze-dried. The nano-micelle size was obtained from DLS. The morphology and micelle size were further characterized using TEM. Platinum content and drug loading efficiency of the nanoparticles was determined by ICP-OES.

Platinum release from polymer/canthaplatin micelles. 2 mg of lyophilized polymer/canthaplatin micelles (Pt content: 11.4 wt%) was dissolved in 2 mL of buffered solution (100 mM PBS, pH = 7.4). The solution was then placed into a pre-swollen dialysis bag with a molecular weight cutoff of 3 kDa and immersed into 18 mL buffered solution. The dialysis was conducted at 37 °C in a shaking culture incubator. 0.5 mL of sample solution was withdrawn from the incubation medium at specified time intervals and measured for Pt concentration by ICP-OES. After sampling, equal volume of fresh buffered solution was immediately added into the incubation medium. The platinum released from the micelles was expressed as the percentage of cumulative platinum outside the dialysis bag to the total platinum in the micelles.

In vitro studies

Cell culture. Lung carcinoma A549 cells and cisplatin resistant A549/DDP cells were purchased from Institute of Biochemistry and Cell Biology, Chinese Academy of Sciences, Shanghai, China, and grown in DMEM (Life Technologies) supplemented with 0.03% L-glutamine and 1% penicillin/streptomycin in 5% CO_2 at 37 °C. A549/DDP cells were maintained with 2 μg/mL of cisplatin. For MTT and other assays, the resistant cells were cultured in cisplatin-free medium for 10 days before conducting cytotoxicity assay.

PP2A activity assay. 5×10^5 cells A549 cells were seeded into six-well tissue culture plates and incubated overnight under standard growth conditions. The media for the cell lines were then replaced by fresh growth media with and without a cisplatin, LB, canthaplatin and polymer/canthaplatin micelles with a Pt or LB content of 5 μM. After 3 h (a duration sufficient for drug uptake, but insufficient for post exposure modification or cell death), cells were washed 3 times in a 0.9% normal saline solution. Tissue protein extraction reagent (T-PER) (CWBiotec) solution was added to cells for protein extraction. Lysates from each treatment group were assayed using a Malachite Green Phosphatase assay specific for serine/threonine phosphatase activity (Ser/Thr phosphatase assay kit; Invitrogen). The relative activity of PP2A was calculated according to the following equation: PP2A activity = (mean experimental phosphate amount / mean control phosphate amount) ×100 (%).

MTT assay. The cytotoxicity of drugs was evaluated by a MTT assay following a published protocol.[27] Cells were seeded in 96-well plates at a density of 4×10^3 cells per well and incubated in DMEM overnight. The medium was then replaced by cisplatin, canthaplatin, polymer/canthaplatin micelles at a final Pt concentration from 1.68 to 108 μM. The incubation was continued for 48 h or 72 h. Then, MTT solution (20 μL) in PBS (5 mg/mL) was added and the plates were incubated for another 4 h at 37 °C, followed by removal of the culture medium containing MTT and addition DMSO (150 μL) to each well to dissolve the formazan crystals formed. Finally, the plates were shaken for 10 min, and the absorbance of formazan product was measured at 490 nm by a microplate reader. Treatment groups for each cell line were replicated three times.

Annexin-V assay. 5×10^5 cells for each cell line (A549, A549/DDP) were seeded into six-well tissue culture plates and incubated overnight under standard growth conditions. The media for the cell lines were then replaced by fresh growth media with and without cisplatin, canthaplatin and polymer/canthaplatin micelles with a Pt content of 10 μM. Treatment groups for each cell line were replicated three times. Cells were then incubated for 48 h at 37 °C and harvested with 0.25% trypsin-EDTA. Cells were washed with PBS and subsequently stained by annexin-V in accordance to the manufactures protocol. Flow cytometry was performed on a BD LSR II flow cytometer (BD Biosciences) and data were analyzed on BD FACSDiva.

Cellular uptake. 5×10^5 cells for each cell line (A549, A549/DDP) were seeded into six-well tissue culture plates and incubated overnight under standard growth conditions. Then the cells were treated with cisplatin, canthaplatin or polymer/canthaplatin micelles with a Pt content of 50 μM for 6 h at

37 °C. To quantitatively determine Pt uptake by cells, the cell samples were washed three times with ice-cold PBS to remove surface-bound drugs first, and then lysed by adding 200 μL cell lysis buffer (Beyotime Institute of Biotechnology, Shanghai, China). 100 μL of the cell lysis solution for each sample was used directly to measure the Pt content by ICP-MS. The other 100 μL of the cell lysis solution was used to determine the protein content in each cell sample by using bicinchoninic acid (BCA) protein assay kit (Beyotime Institute of Biotechnology, Shanghai, China). The platinum content was expressed as microgram of Pt per milligram of total proteins. All experiments were repeated three times.

Repair of DNA-Pt adduct. A549 cells and A549/DDP cells were seeded in six-well tissue culture plates at a density of 5×10^5 cells per well and incubated in DMEM overnight. Cells pre-treated with cispaltin, canthaplatin and polymer/canthaplatin micelles with a Pt content of 50 μM for 6 h were washed three times with ice-cold PBS and frozen at -80 °C (zero time control) or re-incubated in drug-free medium for 1, 2, 4, 8 and 24 h to allow for DNA repair. After the repair incubations, cells were washed twice with cold PBS and again frozen at -80 °C until DNA was isolated and quantified using DNA extract reagent (Qiagen). The total DNA bound platinum was estimated by ICP-MS. The platinum content was expressed as nanogram of Pt per milligram of total DNA. Repair of DNA-Pt adduct was calculated by comparing the platinum content of the repair samples with that in the zero time control. All experiments were repeated three times.

In vivo experiments

Animal use. Kunming (KM) mice (6 - 8 weeks old), and Nude BALB/c mice (4 - 6 weeks old) were purchased from Jilin University (Changchun, China). All mice were maintained under required conditions (*e.g.*, pathogen-free condition for nude mice) and had free access to food and water throughout the experiments. Use of them for this study was approved by the Animal Ethics Committee of Changchun Institute of Applied Chemistry, Chinese academy of sciences.

In vivo anticancer efficacy evaluation. A549 or A549/DDP xenografts tumor model were implanted subcutaneously into the right flank of Nude BALB/c mouse (1×10^7 A549 or A549/DDP cells in 0.1 mL). Tumor nodules were allowed to grow to a volume ~100 mm^3 before initiating treatment. Tumor-bearing BALB/c mice were randomly assigned to three groups: (1) saline (n = 5), (2) cisplatin (4 mg/kg) (n = 5), (3) canthaplatin (2.5 mg Pt/kg) (n = 5), (4) polymer/canthaplatin micelles (2.5 mg Pt/kg) (n = 5), where n is the number of mice in each group. Tumor length and width were measured with calipers, and the tumor volume was calculated using the following equation: tumor volume = length × width × width/2.

Prior to treatment, all the mice were numbered using ear tags, and their weight and the initial tumor volume were measured and recorded. Test animals received three intravenous injections on days 0, 4 and 7 and the injection volume was 200 μL. The weight and tumor volume of each mouse were measured every two days over a period of ~ 30 d.

PP2A activity assay. PP2A activity was assayed in A549 xenografts bearing Nude BALB/c mice. After a single intravenous injection of 0.1 mL of canthaplatin or polymer/canthaplatin micelles with a Pt content of 1 mg/kg, the tumor tissues at different time (0 h, 2 h, 4 h, 8 h, 16 h, 24 h, and 3 mice for each group) after injection were collected, and then tissue protein extraction reagent solution was added for protein extraction. Lysates from each treatment group were assayed for PP2A activity.

Bio-distribution and excretion study. The blood persistence properties of canthaplatin and polymer/canthaplatin micelles were determined using tumor-bearing KM mice. The animals, three per group, were injected in the tail vein with 0.1 mL of canthaplatin and polymer/canthaplatin micelles with a Pt content of 1 mg/kg. At predetermined time intervals, blood samples were collected in pre-weighed heparinized tubes. The percentage of Pt was calculated by taking into consideration that blood constitutes 7% of body weight. Major tissues including heart, liver, spleen, lung, kidney and tumor were also collected and washed with 0.9% saline before weighted. All the tissues were treated with concentrated nitric acid on heating, to obtain clear solutions. The platinum contents in the solutions were determined by ICP-MS and the contents in each tissue were subsequently calculated.

Toxicity evaluation. KM mice were used to evaluate the maximum tolerated dose (MTD) of cisplatin, canthaplatin, and polymer/canthaplatin micelles. All groups (n = 3) received a single dose by intravenous injection. Four groups of mice received cisplatin at a dose of 1, 3, 5, 10 mg/kg. Five groups of mice received either canthaplatin or polymer/canthaplatin micelles with a Pt content of 1, 3, 5, 10 and 15 mg/kg. The control groups received 10, 20, 40, 80, and 100 mg/kg of empty polymer micelles. The injection volume was 0.2 mL in all cases. The weight and physical states of all mice were monitored for a period of 15 d.

After that the blood sample of each mouse was collected from the retro-orbital plexus into a coagulation-promoting tube (Shandong Nanyou Medical appliance, China), and then centrifuged at 3000 rpm for 5 min to obtain plasma samples for measuring clinic parameters including urea nitrogen (UREA), creatinine (CREA), uric acid (UA), alanine aminotransferase (ALT), aspartate aminotransferase (AST) by an automatic biochemical analyzer (Mindray BS-220, China), and white blood concentration (WBC) by an automatic blood counter system (ABX Micros 60, France).

Statistical analysis. The data were expressed as mean ± standard deviation (SD). Student's t-test was used to determine the statistical difference between various experimental and control groups. Differences were considered statistically significant at a level of $p < 0.05$.

Results and discussion

Synthesis and characterization of canthaplatin

Ordinary combination of cisplatin and LB has several potential problems. The different solubility of cisplatin and LB in water makes it difficult to obtain a homogenous injectable solution. Even worse, the severe side effects from cisplatin still remain. Our tactic is to employ a novel inert platinum (IV) compound by tethering LB to cisplatin (to give a new compound named canthaplatin) (Scheme 1).

Direct acylation of *cis,cis,trans*-$Pt(NH_3)_2Cl_2(OH)_2$ with an excess of LB chloride as reported method failed to give canthaplatin, because the Boc group of LB was proved to be unstable to the free HCl in the acylation system.[28] Acylation of *cis,cis,trans*-$Pt(NH_3)_2Cl_2(OH)_2$ using LB anhydride was also unsuccessful. Alternatively, the synthesis of canthaplatin was achieved via a two-step reaction process. Precursor DMC-Pt-DMC was obtained by ring-open reaction of DMC with *cis,cis,trans*-$Pt(NH_3)_2Cl_2(OH)_2$,[26] which was further condensed with BOC-piperazine subsequently to give canthaplatin. By controlling and optimizing reaction conditions, the target compound can be readily isolated in moderate yield when CDI was used as the condensation agent. FTIR, ESI-MS, ^{1}H NMR and elemental analysis confirmed the structure of canthaplatin (Fig. S1-S3, Table S1). Cisplatin (II) and LB fragments were detected by ESI-MS (Fig. S4) under the mimical cancer cell environment (Ascorbic acid concentration is 5-10 mM),[29] which verified our hypothesis that canthaplatin could be reduced to cisplatin(II) and LB in cancer cells to act its dual killing mechanisms.

Preparation and drug release of polymer/canthaplatin micelles

Pt (II) complexes are typically kinetically labile. An impetus for investigating Pt (IV) pro-drugs is their kinetic inertness of more prominence.[30] This reduced reactivity is expected to translate into sustained circulation *in vivo* during which the masked Pt (II) pharmacophore remains safe from deactivation by biological nucleophiles. Only upon entering the reducing environment of cancer cell is the complex supposed to be reduced, releasing the active Pt (II) agent.[31] We propose that nanomicelles encapsulation provides the guest platinum complex an additional degree of protection from reductants and nucleophiles by physically preventing interaction between these agents and the encapsulated platinum complex.

The interior of nanoparticles is more hydrophobic than their surface. Synthesis of Pt (IV)-encapsulated nanoparticles requires that the Pt (IV) host be sufficiently soluble in organic solvents like acetonitrile and DMF. Canthaplatin dissolves in acetonitrile (10 mg/ml), making it a suitable candidate for encapsulation. Polymer/canthaplatin micelles were prepared by nano-precipitation. TEM and DLS were used to characterize the morphology and size of micelles. Platinum content was determined by ICP-MS to be 11.4 wt%. The average loading efficiency was 20%. Results showed that they assumed a spherical shape, the mean diameters were about 70 nm determined by TEM or 82 nm determined by DLS, and no aggregation was observed (Fig. 1a).

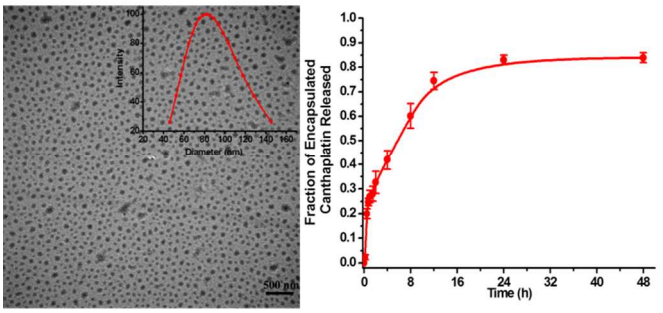

Fig. 1 a) TEM morphology (scale bar = 500 nm) and DLS characterization (inset) of polymer/canthaplatin micelles. b) Platinum release profile of polymer/canthaplatin micelles in PBS solution (pH = 7.4).

Polymer/canthaplatin micelles are actually pro-drugs of cisplatin (II) and LB. Only when canthaplatin escapes from the micelles and is reduced to bioactive fragments, can it act as antitumor agent. Since canthaplatin is physically dispersed throughout the hydrophobic core of the PEG-*b*-PLGA micelles, the release of

canthaplatin should be a slow, diffusion-controlled process. We studied platinum release by dialysis with the polymer/canthaplatin micelles against PBS at pH 7.4 to mimic physiological condition. The amount of platinum released from the micelles was measured by ICP-OES and shown in Fig. 1b. An initial burst release during the first 1 h represents nearly 20% of the total platinum. Thereafter, a period of controlled platinum release occurs, reaching a value of 80% after 48 h. The sustained release behavior confirmed that canthaplatin is a suitable candidate for building a drug loaded nanoparticle.

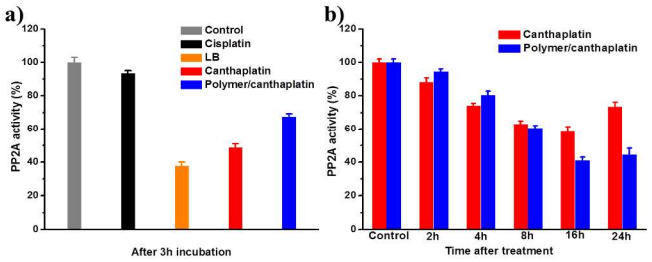

Fig. 2 PP2A activity in a) A549 cells after 3h incubation of drugs and b) A549 xenografts bearing BALB/c mice at different time after *i.v.* injection of drugs (1 mg Pt/kg). Data are expressed as mean ± standard deviation (n = 3).

The release of LB was indirectly evaluated with a PP2A activity assay. As shown in Fig. 2, it was found that the PP2A activity level in A549 cells exposed to LB for 3 h decreased to 37.8% of the control level, while those exposed to canthaplatin and polymer/canthaplatin micelles decreased to 48.5% and 67.3%, respectively. Also *in vivo*, canthaplatin induced 41.6% inhibition of PP2A activity of A549 tumor tissues after 16 h, whereas polymer/canthaplatin micelles exhibited sustaining inhibition of PP2A to 44.4% of control level even after 24 h. The reduced PP2A activity level clearly proved that canthaplatin and LB molecules could be controlled release from the polymer/canthaplatin micelles and still possess the capability to inhibit PP2A function.

Effect of polymer/canthaplatin micelles on cisplatin resistance in vitro

As above mentioned, reduced drug uptake and DNA repair are the two main mechanisms of cisplatin resistance. Previous reports have demonstrated that polymeric nano-carriers would have the chance to improve the intracellular drug delivery.[32] And suppression of PP2A activity would have inhibitory effect on DNA repair, since PP2A is a ubiquitous expressed protein essential for nucleotide excision repair (NER) and DNA damage-induced defense mechanism.[33,34] Fortunately, the characteristics of PP2A inhibition and polymer encapsulation which were attached to canthaplatin provided us an excellent opportunity and a platform to promote deeper investigation on anti-cancer efficacy especially in cisplatin-resistant cancer cells. The cytotoxicity of cisplatin, canthaplatin and polymer/canthaplatin micelles was assayed using lung cancer cells A549 and cisplatin resistant cells A549/DDP (Table 1, S3). A549/DDP cells clearly showed resistance to cisplatin: the IC_{50} value of cisplatin in A549/DDP cells (61.2 μM) was much higher than that in A549 cells (3.6 μM) at 72 h, representing a resistant factor (RF) of 17 (Table 1, Fig. 3a). As expected, canthaplatin itself was more susceptive than cisplatin in A549/DDP cells (31.9 μM), and the resistant factor was significantly reduced (RF = 2.2) (Fig. 3b). It was exciting to find that the cytotoxicity of the polymer/canthaplatin micelles was the highest in A549/DDP cells at 72 h, and the resistant factor was further reduced to 1.4 (Fig. 3c). These results suggested that canthaplatin may overcome acquired resistance to cisplatin to some extent, and polymer encapsulation could further enhance this ability. An annexin-V assay was performed to further determine the percentage of apoptotic cells after exposure to cisplatin, canthaplatin, or polymer/canthaplatin micelles in A549 cells and A549/DDP cells (Fig. 4). Cisplatin evoked severe apoptosis in A549 cells (65.3%), but low level of apoptosis in A549/DDP cells (9.0%). On the contrary, polymer/canthaplatin micelles could induce more A549/DDP cells apoptosis (48.9%) compared to canthaplatin (14.4%) and cisplatin, showing good accordance to the MTT results. All these data suggested that polymer/canthaplatin micelles possess excellent capacity to overcome cisplatin resistance.

Table 1 Representative IC_{50} values and Pt uptake of cispaltin, canthaplatin and polymer/canthaplatin micelles.

Drugs	IC_{50} (μM of Pt)				Pt uptake (μg Pt/mg protein)	
	A549		A549/DDP		A549	A549/DDP
	48 h	72 h	48 h	72 h	6 h	
Cisplatin	6.3 ± 1.0	3.6 ± 0.6	87.3 ± 4.9	61.2 ± 3.7	94.05 ± 3.4	43.98 ± 2.9
Canthaplatin	26.4 ± 4.2	14.4 ± 3.3	51.8 ± 4.0	31.9 ± 2.5	249.91 ± 1.5	281.6 ± 2.7
Polymer/canthaplatin	22.7 ± 2.8	12.1 ± 3.7	36.2 ± 3.6	17.4 ± 3.0	678.74 ± 4.1	732.17 ± 3.5

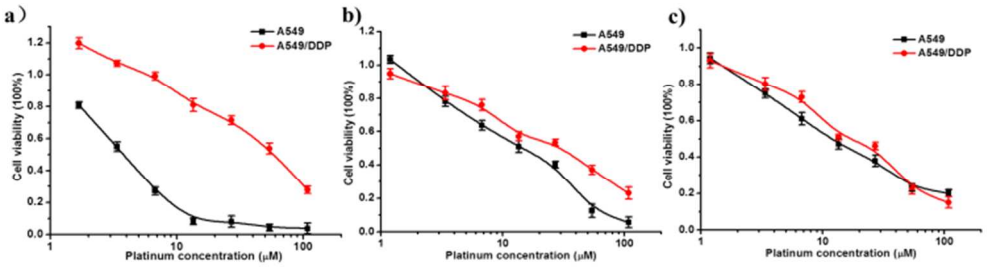

Fig. 3 Cell viability curves of a) cispaltin, b) canthaplatin and c) polymer/canthaplatin micelles against A549 and A549/DDP cells for 72 h.

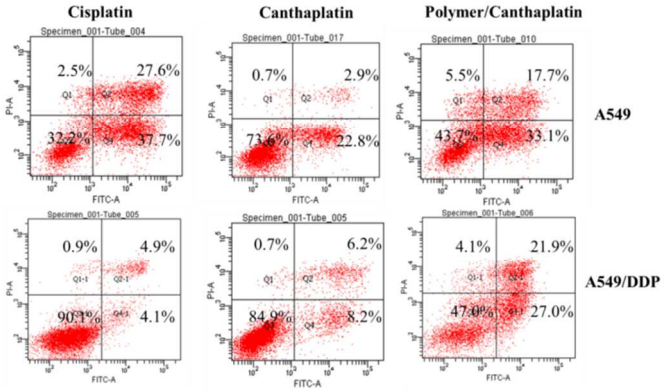

Fig. 4 Apoptosis induced against A549 and A549/DDP cells by canthaplatin, cisplatin and polymer/canthaplatin after 48 h incubation using an annexin-V assay.

The enhanced anti-cancer activity of polymer/canthaplatin micelles is believed to be a result of the polymeric decoration and dual action modes of canthaplatin. Therefore, cellular platinum uptake assay was performed firstly to compare the drug amounts internalized by cells. The results are shown in Table 1. It was found that after 6 h cisplatin incubation, the Pt uptaken by both A549 and A549/DDP cells were in low levels. And the Pt uptaken by A549/DDP cells (43.98 μg Pt/mg protein) was much less than that by A549 cells (94.05 μg Pt/mg protein), implying the cisplatin resistant character of A549/DDP cells. Compared to cisplatin, increased drug cellular uptake was found in both A549 cells (249.91 μg Pt/mg protein) and A549/DDP cells (281.6 μg Pt/mg protein) in canthaplatin group which may be attributable to its lipophilicity efficiency. It is noteworthy that after polymeric decoration of canthaplatin, the Pt uptaken from polymer/canthaplatin micelles in A549 and A549/DDP cells were significantly increased to 678.74 and 732.17 μg Pt/mg protein, respectively. All these results indicated that polymeric decoration of canthaplatin exhibited enhanced drug accumulation in cancer cells, providing a physical foundation for cisplatin resistance reversal. It is reasonable that nanoparticles may re-activate the defective endocytosis and avoid the reduced uptake caused by the low expression of copper transport protein Ctr1 in resistant cells, to achieve the enhanced drug accumulation.[35-37]

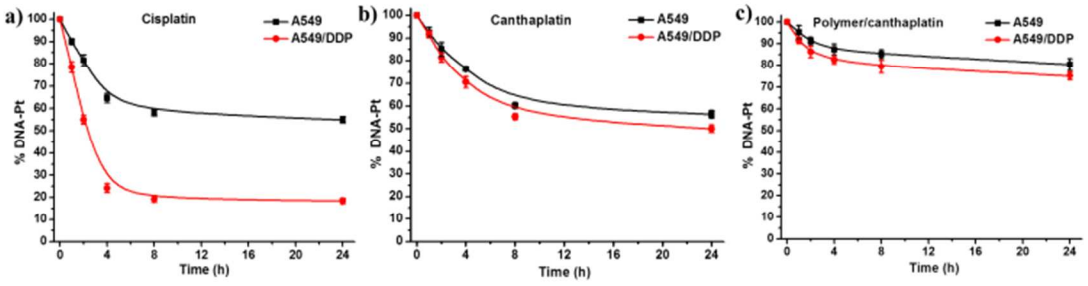

Fig. 5 DNA-Pt adduct repair with time in A549 and A549/DDP cells after 6 h pre-incubation (time = 0 h) of a) cisplatin, b) canthaplatin and c) polymer/canthaplatin micelles.

Cisplatin attacks nuclear DNA, leading to DNA damage by intra-strand cross-links (DNA-Pt adducts). And repair of damaged DNA, like removal of DNA-Pt adducts, is the main mechanism of tumor resistance to cisplatin. Since PP2A is essential for nucleotide excision repair which is the main manner of DNA repair mechanism in cisplatin resistant cells, the effects of PP2A inhibition on DNA repair was also determined to further understand the cell mechanism of cisplatin resistance reversal induced by polymer/canthaplatin micelles. In the DNA repair assays (Fig. 5), after 6 h pre-incubation of drugs with cancer cells to form DNA-Pt adducts (Table S2), 18.2% and 45.5% of the adducts were removed within the first 2 h in A549 and A549/DDP

cells for cisplatin treatment, and the removal amount of DNA-Pt adducts after 24 h were further increased to 45.1% and 81.6%, respectively. However, there was no significant difference in the rate of removal for canthaplatin and polymer/canthaplatin micelles, showing improved sensitivity of these drugs to cisplatin-resistant cells (A549/DDP). Even compared with small anti-resistance drug canthaplatin, the DNA-Pt adducts removal of polymer/canthaplatin micelles group in A549/DDP cells within 24 h was extremely reduced to less than 20%. These results clearly indicated that polymer/canthaplatin micelles have satisfying character to diminish DNA repair by PP2A inhibition and overcome cisplatin resistance.

In vivo evaluation on cisplatin resistance of polymer/canthaplatin micelles

To further prove the drug ability to overcome cisplatin resistance, we evaluated the antitumor activity of polymer/canthaplatin micelles *in vivo* against subcutaneous A549 and A549/DDP tumors developed by injection of tumor cells in the flank of BALB/c nude mice. The following regimens were administered by intravenous drug injection for three times in one week: (i) saline, (ii) cisplatin (4 mg/kg), (iii) canthaplatin (2.5 mg Pt /kg), and (iv) polymer/canthaplatin micelles (2.5 mg Pt /kg). We aimed to determine whether delivery of the pro-drug, canthaplatin with polymeric nanomicelles will result in enhanced antitumor efficacy *in vivo* when compared to free cisplatin given in its conventional dosage form. The results showed that administration of cisplatin exhibited good efficiency to restrict A549 tumor (Fig. 6a), but failed to inhibit the growth of A549/DDP tumors and in consequence the tumor volume increased to about 500 mm^3 after 4 weeks (Fig. 6c), which verified the tumors resistance to cisplatin of A549/DDP model. Interestingly, administration of canthaplatin exhibited a lower efficiency than cisplatin in A549 tumors but a better efficiency in A549/DDP tumors, corresponding to the *in vitro* results. As expected, polymer/canthaplatin micelles exhibited high antitumor activity in both tumor xenograft models. Especially in A549/DDP tumor model, polymer/canthaplatin micelles successfully overcame the cisplatin resistance of A549/DDP cells with substantial restricted tumor growth, and the tumor size decreased to about 30 mm^3 after 4 weeks. The present technology differs in two distinct ways, which in combination may explain our observed improvement in drug therapeutic index. Foremost, we delivered the two synergetic drugs, cisplatin and LB in form of a Pt(IV) pro-drug which is more susceptive than cisplatin to cisplatin resistant tumor. In addition, we employed a polymeric delivery vehicle, which we and others have shown to improve drug efficacy.[9-16, 22, 38-41]

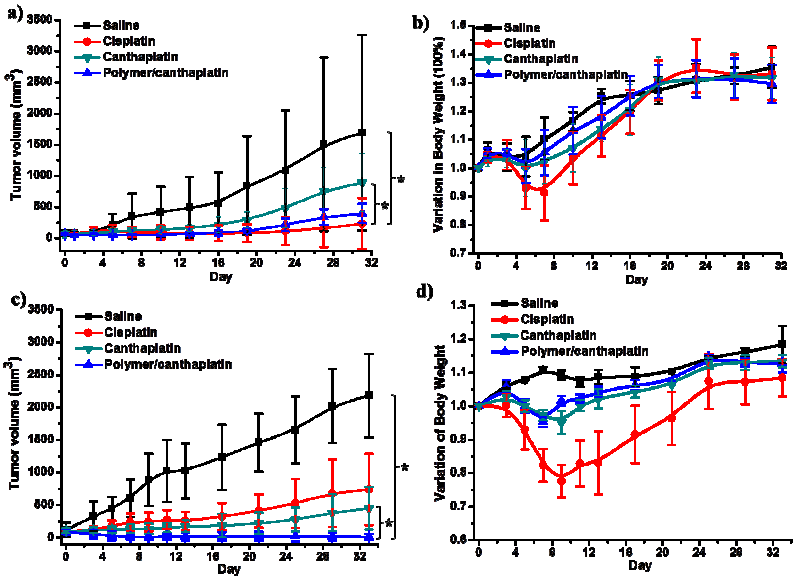

Fig. 6 Tumor growth inhibition curves (a, c) and body weight change profiles (b, d) of female BALB/c nude mice bearing A549 xenografts (a, b) and A549/DDP (c, d) xenografts after saline, cisplatin (4 mg/kg), canthaplatin (2.5 mg Pt/kg) and polymer/canthaplatin micelles (2.5 mg Pt/kg) intravenous injection on days 0, 3, and 7. Data are expressed as mean ± standard deviation, n = 5, $*P < 0.05$.

Body weight was also monitored to evaluate the *in vivo* toxicity of the drugs. Administration of free cisplatin led to significant body weight loss in both A549 and A549/DDP mice during the first 10 days while administration of canthaplatin and polymer/canthaplatin

micelles showed little side effect on body weight growth of mice, indicating a relieved toxicity of the pro-drug and drug system (Fig. 6b, d). We also found that polymeric encapsulation of canthaplatin resulted in a significant prolongation of Pt presence in blood (Fig. S5), and reduced accumulation of Pt in liver and kidney while increased accumulation in tumor through the EPR effect, indicating the reduced nephrotoxicity and hepatotoxicity after administration of polymer/canthaplatin micelles (Fig. S6). The *in vivo* toxicity was further evaluated by examining the maximum tolerated dose (MTD) and alterations of clinical chemistry parameters in KM mice after treatment with polymer/canthaplatin micelles, canthaplatin and cisplatin. MTD was estimated based on the threshold at which dose all animals survived (Table S3). From the results, we conclude that MTD for polymer/canthaplatin micelles is 10 mg Pt/kg, and that for cisplatin is 5 mg/kg and canthaplatin is 5 mg Pt/kg. Polymer/canthaplatin micelles appeared to be better tolerated than cisplatin in its conventional dosage form. As shown in Fig. 7, the level of clinical chemistry parameters including UA, UREA, CREA, AST and ALT were increased for groups treated with cisplatin at a dose of 5 mg/kg, indicating the appearances of severe renal toxicity and hepatotoxicity. However, these toxicities were significantly relieved in treatment with high doses of polymer/canthaplatin micelles, showing clear advantage in safety. No significant differences were observed between the groups treated with canthaplatin and polymer/canthaplatin micelles. Meanwhile, the analysis of white blood count (WBC) showed that treatment with polymer/canthaplatin micelles led to minimal decrease in WBC, indicating the lowest effect on immune systems after chemotherapy. These results revealed significant differential toxicity profiles for polymer/canthaplatin micelles and cisplatin as well as the beneficial effects of polymeric micelles in reducing its commonly encountered toxicities.

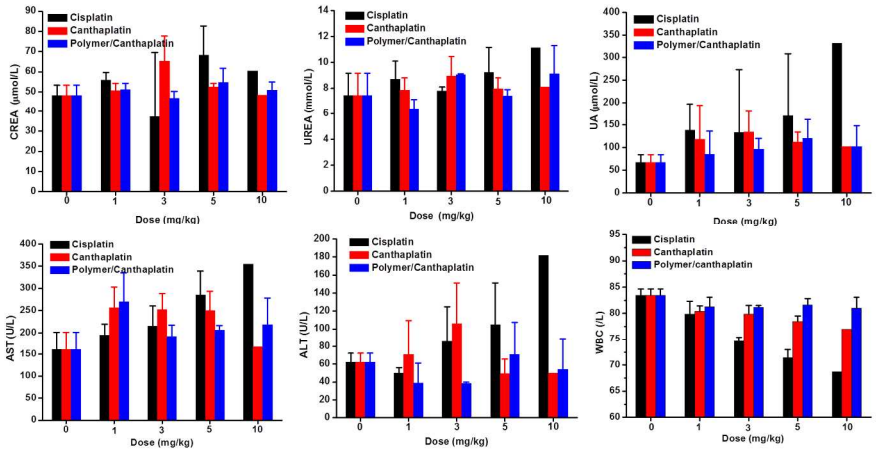

Fig. 7 Alterations of UREA, CREA, UA, ALT, AST and WBC in KM mice after treatment with various doses of cisplatin, canthaplatin and polymer/canthaplatin micelles. Data are expressed as mean ± standard deviation.

Conclusions

In the present investigation, a Pt (IV) pro-drug of cisplatin and a PP2A inhibitor LB, canthaplatin, was designed and delivered using PEG-*b*-PLGA micelles for combination chemotherapy. Polymer/canthaplatin micelles facilitated the delivery of drugs into cancer cell through endocytosis and diminished DNA repair by PP2A inhibition, resulting in enhanced anti-tumor efficiency and excellent reversal ability on tumor resistance to cisplatin both *in vitro* and *in vivo*. Additionally, polymer/canthaplatin micelles could prolong drug residence in blood and decrease the side effects when compared to that of cisplatin. Our studies avoid the drug resistance and side effects that affect the use of cisplatin *in vivo*, and would have broad implication for cancer therapy given the relatively ubiquitous use of cisplatin in oncology. We also suggest that similar strategies could be undertaken to combine Pt (IV) pro-drugs with polymeric co-delivery system to synergistically improve efficacy and safety.

Acknowledgements

The authors would like to thank the financial support from National Natural Science Foundation of China (No. 51403198, 51321062 and 21174143), Ministry of Science and Technology of China (863 Project, No. SS2012AA020603), and “100 Talents Program” of Chinese Academy of Sciences (No.KGCX2-YW-802).

Notes and references

[a] *State Key Laboratory of Polymer Physics and Chemistry, Changchun Institute of Applied Chemistry, Chinese Academy of Sciences, Changchun, 130022, PR China*
[b] *University of Chinese Academy of Sciences, Beijing 100049, PR China*
[c] *Key Laboratory of Polymer Ecomaterials, Changchun Institute of Applied Chemistry, Chinese Academy of Sciences, Changchun 130022, PR China*
**Correspondence author. Tel & Fax: +86-431-85262769; E-mail: ybhuang@ciac.ac.cn*

Electronic Supplementary Information (ESI) available: FTIR, ESI-MS, ^{1}H NMR, elemental analysis characterization and ligand exchange reactions of canthaplatin, details of DNA-Pt adducts formation, bio-distribution and excretion study results, dosing information for MTD studies in KM mice can be found in the online version.

1. B. Rosengerg, L. VanCamp, J. E. Trosko and V. H. Mansour, Nature, 1969, **222**, 385–386.
2. M. Galanski, M. A. Jakupec and B. K. Keppler, Curr. Med. Chem., 2005 **12**, 2075–2094.
3. V. Pinzani, F. Bressolle, I. J. Haug, M. Galtier, J. P. Blayac and P. Balmhs, Cancer Chem. Pharm., 1994, **35,** 1–9.
4. N. Eckstein and J. Exp. Clin. Cancer Res., 2011, **30**, 91.
5. X. Wang and Z. Guo, Chem. Soc. Rev., 2013, **42**, 202–224.
6. H. S. Oberoi, N. V. Nukolova, A. V. Kabanov and T. K. Bronich, Adv. Drug Deliv. Rev., 2013, **65**, 1667–1685.
7. S. Dhara and S. J. Lippard, Proc. Natl. Acad. Sci. U. S. A., 2009, **106**, 22199 –22204.
8. W. H. Ang, I. Khalaila, C. S. Allardyce, L. Juillerat-Jeanneret and P. J. Dyson, J. Am. Chem. Soc., 2005, **127**, 1382–1383.
9. H. Xiao, H. Song, Q. Yang, H. Cai, R. Qi, L. Yan, S. Liu, Y. Zheng, Y. Huang and T. Liu, Biomaterials, 2012, **33**, 6507–6519.
10. N. Kolishetti, S. Dhar, P. M. Valencia, L. Q. Lin, R. Karnik, S. J. Lippard, R. Langer and O. C. Farokhzad, Proc. Natl. Acad. Sci. U. S. A., 2010, **107**, 17939–17944.
11. X. Y. Xu, K. Xie, X. Q. Zhang, E. M. Pridgen, G. Y. Park, D. S. Cui, J. J. Shi, J. Wu, P. W. Kantoff and S. J. Lippard, Proc. Natl. Acad. Sci. U. S. A., 2013, **110**, 18638−18643.
12. D. Zhou, H. Xiao, F. Meng, S. Zhou, J. Guo, X. Li, X. Jing and Y. Huang, Bioconjugate Chem., 2012, **23**, 2335−2343.
13. T. C. Johnstone, N. Kulak, E. M. Pridgen, S. J. Lippard, R. Langer and O. C. Farokhzad, ACS NANO, 2013, **7**, 5675−5683.
14. H. Xiao, W. Li, R. Qi, L. Yan, R. Wang, S. Liu, Y. Zheng, Z. Xie, Y. Huang and X. Jing, J. Control. Release, 2014, **163**, 304-314.
15. L. Zhang, C. M. J. Hu, V. Fu and S. Aryal, J. Mater. Chem., 2012, **22**, 994−999.
16. S. Dhar, N. Kolishetti, S. J. Lippard, C. Omid and O. C. Farokhzad, Proc. Natl. Acad. Sci. U. S. A., 2011, **108**, 1850−1855.
17. D. Wang and S. J. Lippard, Nat. Rev. Drug Discov., 2005, **4**, 307−320.
18. R. P. Wernyj and P. J. Morin, Drug Resist. Updates, 2004, **7**, 227−232.
19. M. Ohmichi, J. Hayakawa, K. Tasaka, H. Kurachi, Y. Murata and Trends Pharmacol. Sci., 2005, **26**, 113−116.
20. L. P. Martin, T. C. Hamilton and R. J. Schilder, Clin. Cancer Res., 2008 **14**, 1291−1295.
21. A. F. Miguel, A. Carlos and M. P. Jose, Chem. Rev., 2003, **103**, 645–662.
22. D. Zhou, H. Xiao, F. Meng, X. Li, Y. Li, X. Jing and Y. Huang, Adv. Healthcare Mater., 2013, **2**, 822–827.
23. J. Lu, J. S. Kovach, F. Johnson, J. Chiang, R. Hodes, R. Lonser and Z. P. Zhuang, Proc. Natl. Acad. Sci. U. S. A., 2009, **106**, 11697–11702.
24. C. Zhang, Y. Peng, F. Wang, Xu. Tan, N. Liu, Song. Fan, D. Wang, L. Zhang, D. Liu, T. Wang, S. Wang, Y. Zhou, Y. Su, T. Cheng, Z. Zhuang and C. Shi, Biomaterials, 2010, **31**, 9535−9543.
25. J. S. Kovach and F. Johnson, U.S. Patent, No.7998957B2, 2011.
26. M. R. Reithofer, S. M. Valiahdi, M. Galanski, M. A. Jakupec, V. B. Arion and B. K. Keppler, Chem. Biodivers., 2008, **5**, 2160−2170.
27. J. Guo, Y. Wei, D. Zhou, P. Cai, X. Jing, X. Chen and Y. Huang, Biomacromolecules, 2011, **12**, 737–746.
28. M. Galanski and B. K. Keppler, Inorg. Chem., 1996, **35,** 1709−1711.
29. S. S.M. Hassan and G. A. Rechnitz, Anal. Chem., 1982, **54**, 1972−1976.
30. M. D. Hall, H. R. Mellor, R. Callaghan and T. W. Hambley, J. Med. Chem., 2007, **50**, 3403–3411.
31. M. D. Hall, T. W. Hambley, Coord. Chem. Rev., 2002, **232**, 49–67.
32. T. Doane and C. Burda, Adv. Drug Deliv. Rev., 2013, **65**, 607–621.
33. M. Herman, Y. Ori, A. Chagnac, T. Weinstein, A. Korzets, D. Zevin, T. Malachi and U. Gafter, J. Lab. Clin. Med., 2002, **140**, 255–262.
34. R. R. Ariza, S. M. Keyse1, J. G. Moggs and R. D. Wood, Nucl. Acids Res., 1996, **24**, 433–440.
35. M. Murakami, H. Cabral, Y. Matsumoto, S. Wu, M.R. Kano, T. Yamori, N. Nishiyama and K. Kataoka, Sci. Transl. Med., 2011, **3**, 64ra2.
36. X. Liang, H. Meng, Y. Wang, H. He, J. Meng, J. Lu, P.C. Wang, Y. Zhao, X. Gao, B. Sun, C. Chen, G. Xing, I. Shen, M.M. Gottesman, Y. Wu, J. Yin and L. Jia, Proc. Natl. Acad. Sci. U. S. A., 2010, **107**, 7449–7454.
37. Y. Min, C. Mao, S. Chen, G. Ma, J. Wang and Y. Liu, Angew. Chem. Int. Ed., 2012, **51**, 1–7.
38. H. Maeda, J. Wu, T. Sawa, Y. Matsumura and K. Hori, J. Control. Release, 2000, **65**, 271–284.
39. K. Avgoustakis, A. Beletsi, Z. Panagi, P. Klepetsanis, A. G. Karydas and D. S. Ithakissios, J. Control. Release, 2002, **79**, 123–135.
40. S. P. Abhimanyu, S. Shivani, T. C. Kenneth, C. Padmaparna, W. M. Katherine, B. Julia, W. H. Michael, J. A. Nathan, B. Basar, M. D. Daniela, A. M. Raghunath and S. Shiladitya, Proc. Natl. Acad. Sci. U. S. A., 2010, **107**, 12435–12440.
41. M. Kamimura, T. Furukawa, S. Akiyamac and Y. Nagasaki, Biomater. Sci., 2013, **1**, 361–367.

